Experimental identification and validation of an electrochemical model of a Lithium-Ion Battery

Carmelo Speltino, Domenico Di Domenico, Giovanni Fiengo and Anna Stefanopoulou

***Abstract*— In this work an experimental parameter identification and validation for an electrochemical lithium-ion battery model is illustrated. The model was presented in [2] where, aimed at estimating the battery State Of Charge (SOC), the model was also averaged and an extended Kalman filter based on the average model was designed. The identification procedure is based on experimental data collected from a 6.8 Ah lithium-ion battery during charge and discharge processes. Experimental data are then compared with battery model output for validation purpose. A procedure for SOC calculation is also shown at the end of the article.**

Keywords **- Experimental Identification, Model Validation, Lithium-Ion Battery, SOC Computation.**

GLOSSARY

Symbol	Name	Unit
i_e	electrolyte current density	A cm^{-2}
i_s	solid current density	A cm^{-2}
ϕ_e	electrolyte potential	V
ϕ_s	solid potential	V
c_e	electrolyte concentration	mol cm^{-3}
c_s	solid concentration	mol cm^{-3}
c_{se}	solid concentration at electrolyte interface	mol cm^{-3}
j^{Li}	Butler-Volmer current density	A cm^{-3}
θ_n	normalized solid concentration at anode	-
θ_p	normalized solid concentration at cathode	-
U	open circuit voltage	V
U_n	anode open circuit voltage	V
U_p	cathode open circuit voltage	V
η	overpotential	V
F	Faraday's number	C mol^{-1}
I	battery current	A
R	gas constant	J K^{-1} mol^{-1}
T	temperature	K

TABLE I

LITHIUM-ION MODEL NOMENCLATURE.

I. INTRODUCTION

Lithium-ion batteries play an important role in the area of hybrid vehicle design, scale-up, optimization and control issues of Hybrid-Electrical Vehicles (HEV) as a high-rate transient power source. When batteries operate in a relative limited range of State Of Charge (SOC), high efficiency, slow aging and no damaging are expected. As consequence, the SOC estimation and regulation is one of the important and challenging tasks for hybrid and electrical vehicle power source control.

Several techniques have been proposed for the SOC estimation, reaching an accuracy of about 2% [7], [8]. In order to improve this accuracy, SOC estimation based on electrochemical models has been investigated in [1], [2], [4], [11]. These models are generally preferred to the equivalent circuit, or to other kinds of simplified models, thanks to their ability to predict the physical cells limitations, which have a relevant effect in the automotive application, where the battery suffers very often the stress of very high transient loads [10].

In [1] and [2] the authors of the present work have revised a full order electrochemical model in order to obtain an average model suitable for a feasible solid concentration estimation. The average model reduces the battery model complexity and predicts the solid concentration profile during charge and discharge making possible to realize a real-time on-board SOC estimation with an Extended Kalman Filter (EKF).

In this work, parameter identification and validation of the reduced order model to be used for the EKF estimation of the SOC are presented. The experimental setup used for the data collection is composed of a 6.8 Ah lithium-ion battery, an electronic load of the 3600 series from the Prodigit, a DC voltage generator and a simple voltage-current measurement circuit. Sensor measurements have been collected using a 16-bit ADC from National Instruments. A series of experiments has been conducted on the battery, covering both full charge and discharge according to different power request profiles. The measured current and voltage signals have been utilized respectively as reference input and output in the model identification procedure.

The paper is organized as follows. In section II, the model reduction technique is presented, while in section III and IV the experimental setup and the identification procedure are illustrated in detail. In section V results of validation tests are shown, in order to validate the identified model.

II. BATTERY CELL MODEL

The battery is composed of three main parts: the negative electrode, the separator and the positive electrode. Referring to a battery with porous electrode, each of them consists of a solid matrix inside an electrolyte solution, while the separator is electrolyte solution itself.

The separator is a solid or liquid solution with high concentration of lithium ion. It conducts the ion but it acts as an electronic insulator. At the negative electrode (generally

Carmelo Speltino, Domenico Di Domenico and Giovanni Fiengo are with Dipartimento di Ingegneria, Università degli Studi del Sannio, Piazza Roma 21, 82100 Benevento. E-mail: {carmelo.speltino, domenico.didomenico, gifiengo}@unisannio.it

Anna Stefanopoulou is with Mechanical Engineering Univ of Michigan, Ann Arbor MI 48109-2121. E-mail: annastef@umich.edu. She is funded by NSF CMS-GOALI 0625610.

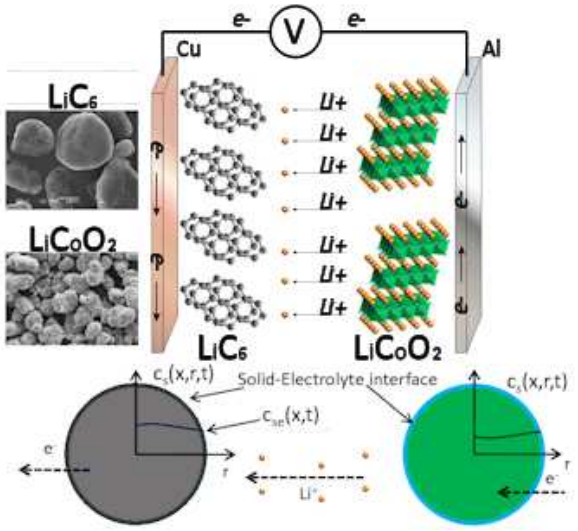

Fig. 1. Schematic macroscopic (x-direction) cell model with coupled microscopic (r-direction) solid diffusion model.

composed of $\mathrm{Li}_x\mathrm{C}_6$), the solid active material particles of lithium diffuse to the electrolyte-solid interface where the chemical reaction occurs, transferring the lithium ions to the solution and the electrons to the collector [10]. The produced electrolyte material flows through the solution to the positive electrode, where, at the interface of the solid material, it reacts and inserts into the metal oxide solid particles.

It's generally accepted that a microscopic description of the battery is intractable, due to the complexity of the interfaces [12]. So, in order to mathematically model the battery, both macroscopic and microscopic physics have to be considered.

The equations used in this paper describe the battery system with four quantities, i.e. solid and electrolyte concentrations (c_s, c_e) and solid and electrolyte potentials (ϕ_s, ϕ_e)(see [5], [10]).

$$\frac{\partial}{\partial x}\left(\kappa^{eff}\overrightarrow{\nabla}_x\phi_e + \kappa_D^{eff}\overrightarrow{\nabla}_x \ln c_e\right) = -j^{Li} \tag{1}$$

$$\frac{\partial}{\partial x}\left(\sigma^{eff}\overrightarrow{\nabla}_x\phi_s\right) = j^{Li} \tag{2}$$

$$\frac{\partial \epsilon_e c_e}{\partial t} = \overrightarrow{\nabla}_x\left(D_e^{eff}\overrightarrow{\nabla}_x c_e\right) + \frac{1-t^0}{F}j^{Li} \tag{3}$$

$$\frac{\partial c_s}{\partial t} = \overrightarrow{\nabla}_r(D_s\overrightarrow{\nabla}c_s) \tag{4}$$

coupled with the Butler-Volmer current density equation

$$j^{Li}(x) = a_s j_0\left[\exp\left(\frac{\alpha_a F}{RT}\eta\right) - \exp\left(-\frac{\alpha_c F}{RT}\eta\right)\right] \tag{5}$$

where the overpotential η is obtained as

$$\eta = \phi_s - \phi_e - U(c_{se}) \tag{6}$$

where $U(c_{se})$ is the open circuit potential, which is an empirical correlation function of the solid concentrations and the coefficient j_0 calculated as

$$j_0 = k_0(c_e)^{\alpha_a}(c_{s,max} - c_{se})^{\alpha_a}(c_{se})^{\alpha_c}. \tag{7}$$

The cell potential is computed as

$$V = \phi_s(x=L) - \phi_s(x=0) - \frac{R_f}{A}I \tag{8}$$

where R_f is the film resistance on the electrodes surface and A is the collectors surface. More details on the model and its parameters can be found in [2], [10], [13].

A model simplification can be achieved by neglecting the solid concentration distribution along the electrode and considering the material diffusion inside a representative solid material particle for each electrode. This simplification introduces an average value for the solid concentration which can be related with the definition of battery state of charge. Furthermore, by assuming high concentration of electrolyte material in the solution, the electrolyte concentration c_e can be considered constant and its average value can be used in the model.

Although these simplifications result in a heavy loss of information, they can be useful in control and estimation applications as we demonstrate next. In accordance with the mean solid concentration, the spatial dependence of the Butler-Volmer current is ignored and a constant value $\bar{j}^{Li}$ is considered which satisfies the spacial integral (for the anode or the cathode)

$$\int_0^{\delta_n} j^{Li}(x)dx = \frac{I}{A} = \bar{j}_n^{Li}\delta_n \tag{9}$$

where δ_n is the anode thickness. This averaging procedure is equivalent to considering a representative solid material particle somewhere along the anode and the cathode [1].

The partial differential equation (4), describes the solid phase concentration along the radius of active particle, but the macroscopic model requires only the concentration at the electrolyte interface.

By using the finite difference method for the spatial variable r, it is possible to express the spherical PDE into a set of ordinary differential equations (ODE), dividing the sphere radius in $M_r - 1$ slices, each of size $\Delta_r = \frac{R_s}{M_r - 1}$ and rewriting boundary conditions [9]. The new system presents $M_r - 1$ states $\mathbf{c_s} = (c_{s_1}, c_{s_2}, ...c_{s_{M_r-1}})^T$, representing radially distributed concentrations at finite element node points $1, ..., M_r - 1$

$$\dot{c}_s = \mathbf{A}c_s + \mathbf{B}\bar{j}^{Li}. \tag{10}$$

where $\mathbf{A}$ is a constant tri-diagonal matrix, function of the diffusion coefficient D_s. The output of the system is the value of the solid concentration at the sphere radius, that can be rewritten as

$$\bar{c}_{se} = c_{s_{M_r-1}} - \mathbf{D}\bar{j}^{Li}. \tag{11}$$

where $\mathbf{D}$ is function of diffusion coefficient D_s and active surface area a_s. Two sets of ODEs, one for the anode and one for the cathode are then obtained. The positive and negative electrode dynamical systems differ at the constant values and at the input sign.

The initial values of $\bar{c}_{se}$ when the battery is fully charged is defined as $\bar{c}_{se,x}^{100\%}$ and when fully discharged as $\bar{c}_{se,x}^{0\%}$,

with $x = p, n$ for the positive and negative electrode. It is convenient to define the normalized concentration, also know as stoichiometry, $\theta_x = \bar{c}_{se,x}/c_{se,max,x}$, with $x = p, n$ for the positive and negative electrode.

The battery voltage (8), using (6) and using the average values at the anode and the cathode, can be rewritten as

$$\begin{aligned} V(t) = (\bar{\eta}_p - \bar{\eta}_n) + \left(\bar{\phi}_{e,p} - \bar{\phi}_{e,n}\right) \\ + (U_p(\theta_p) - U_n(\theta_n)) - \frac{R_f}{A} I. \end{aligned} \tag{12}$$

Using the microscopic current average values and imposing the boundary conditions and the continuity at the interfaces, the solutions of equations (1) - (4) can be found. The results can be found in [2] and [1] and are not reported here for brevity.

Using (5) it is possible to express the overpotentials difference as function of average current densities and solid concentrations as follows

$$\bar{\eta}_p - \bar{\eta}_n = \frac{RT}{\alpha_a F} \ln \frac{\xi_p + \sqrt{\xi_p^2 + 1}}{\xi_n + \sqrt{\xi_n^2 + 1}} \tag{13}$$

where

$$\xi_p = \frac{\bar{j}_p^{Li}}{2 a_s j_{0p}} \quad \text{and} \quad \xi_n = \frac{\bar{j}_n^{Li}}{2 a_s j_{0n}}. \tag{14}$$

The approximate solution for the electrolyte potential at interface with the collectors leads to

$$\bar{\phi}_{e,p} - \bar{\phi}_{e,n} = \phi_e(L) - \phi_e(0) = -\frac{I}{2Ak^{eff}} \left(\delta_n + 2\delta_{sep} + \delta_p\right). \tag{15}$$

Finally, the battery voltage (12) can be rewritten as a function of current demand and average solid concentration

$$\begin{aligned} V(t) = \frac{RT}{\alpha_a F} \ln \frac{\xi_p + \sqrt{\xi_p^2 + 1}}{\xi_n + \sqrt{\xi_n^2 + 1}} \\ + (U_p(\theta_p) - U_n(\theta_n)) - \frac{K_r}{A} I. \end{aligned} \tag{16}$$

where $K_r = \frac{1}{2Ak^{eff}} \left(\delta_n + 2\delta_{sep} + \delta_p\right) + R_f$ is a term that take into account both internal and collector film resistances.

III. Experimental Set-Up

The battery utilized in the experimental set-up is a 37 V - 6.8 Ah polymer lithium-ion battery from SAFT composed of a series of ten MP176065 cells. The battery pack is equipped with minimum protection circuit, in order to not have non-linear behavior caused from cell balancing electronic rather than from the battery itself. The only limitation present is on maximum current demand, limited to 5 A by an internal amperometric fuse. The experiments has been done with lower current demands. In order to collect the battery experimental data during the charge and the discharge, a series of electronic devices has been utilized. The experimental set-up is composed of an electronic load from the 3600 series of Prodigit, a DC voltage generator and a voltage-current sensor coupled to a 16-bit ADC from National Instruments. Figure 2 shows the connection schematics between the battery, load

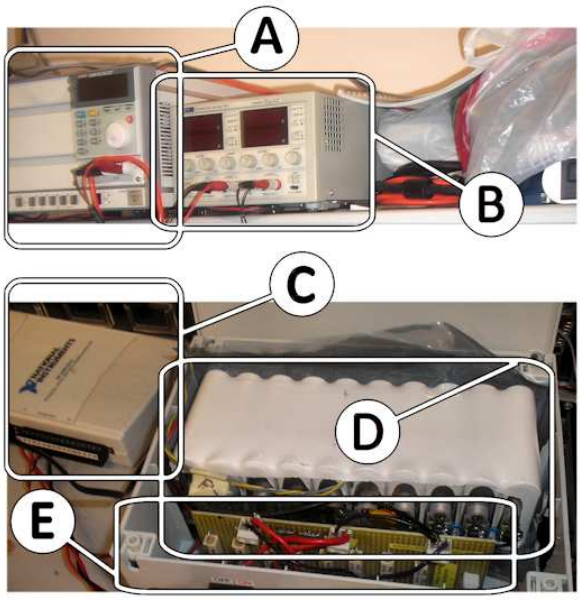

Fig. 2. Experimental set-up: (A) Electronic load, (B) Voltage generator, (C) ADC, (D) Battery and (E) Current and voltage sensor.

and generator, coupled with the voltage/current sensor. The DC voltage generator utilized for the battery charge is a 42 V - 20 A device, able to charge the battery as slow as requested for lithium-ion battery safety concerns and cells balancing. Finally the data has been collected using a 16-bit, 32 channels A/D converter from National Instruments, able to sample the current and voltage signals coming from simple sensors connected to the battery up to 1 MHz. The sampling time has been chosen in a range from 0.1 s to 0.025 s in order avoid oversampling during slow rate experiments or conversely undesired aliasing during faster load dynamics.

IV. Model Identification Procedure

The reduced order model depends on less parameters with respect to the full order one, but this number is still too high to identify the model using all of them as unknowns. Some of the parameters capture geometrical features and some chemical features which can be split into physical and design specific (i.e depend on the particular cell design). In order to reduce the number of parameter to be identified and maintain a good degree of accuracy for model fitting, some values has been taken from literature [10] and some from the cell manufacturer.

The parameters to identify are the maximum positive and negative solid concentration $c_{s,max,p}$ and $c_{s,max,n}$, the positive and negative solid phase diffusion coefficient $D_{s,p}$ and $D_{s,n}$, the positive and negative active surface area per electrode $a_{s,p}$ and $a_{s,n}$, the electrode surface A, the total cell film resistance K_r and the current coefficient k_0 for a total of nine parameters. In addition to these nine parameters it is necessary to know the initial solid concentration values in both electrodes. The discharge and the charge experiments have been conducted with the battery respectively fully charged and fully discharged in order to obtain an estimate

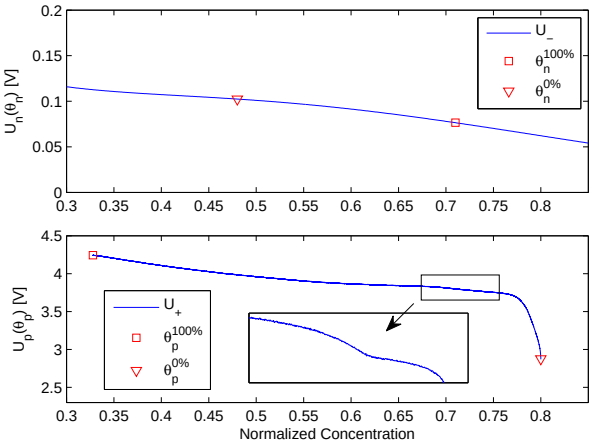

Fig. 3. Empirical open circuit potential correlations for negative and positive electrodes.

for the initial concentration. Literature [4] values provide an initial estimate for the fully charged stoichiometry. These values have been adopted and then refined to fit experimental data.

In order to obtain the correlation between solid concentration inside the electrodes and their open circuit potential, the following procedure has been adopted: from the battery data sheet it is possible to know that the negative electrode active material is composed of graphite (LiC6) so the empirical correlation found in [3] can be utilized, while the positive consists of an unknown mixture of LiCoO2 with other metal oxides. In this case, the specific empirical correlation for $U_p(\theta_p)$ has been established by discharging the cell at a very low constant rate and subtracting $U_n(\theta_n)$ from the measured open circuit voltage.

Figure 3 shows the empirical correlation found for both electrodes. The other battery constants are shown in Table V. The parameter identification procedure has been designed as follows: A set of experimental data has been chosen for the parametric identification routine, comprising charge and discharge process, with constant and pulse current profile, in order to capture both slow and fast dynamics of the battery behavior. In detail, a set of four charges (1 A, 2 A and 3 A at constant current and 4 A with pulse current demand) and four discharges (2 A, 3.5 A and 5 A at constant current and 6 A pulse current demand) have been utilized for parameter identification. Note here that the identification procedure on a single profile leads to a very good fit, but the obtained parameters are tied to the specific experiment and do not fit well other experiments. In order to avoid this local minimum problems and obtain a set of parameters matching different operational points, a global identification procedure has been conducted utilizing all the selected data at the same time. The identification procedure consist in finding the minimum of the following index cost:

$$\min_{par} J = \sum_i \int (V_{M,i}(I_i, par) - V_{REC,i})^2 \qquad (17)$$

where $V_{REC,i}$ is the *i-th* experimental battery voltage measurement corresponding to the *i-th* current demand profile I_i, $V_{M,i}(I_i, par)$ is the model predicted voltage and par is the vector of parameters to identify. In order to obtain a guess starting point for the parameter set, a rough estimation of their values has been obtained coupling literature with battery nominal performances. The minimization procedure has been conducted using Matlab/Simulink, with a gradient free function minimization algorithm specifically suited for non-linear scalar function. The single experiment maximum error tolerance has been fixed around ± 0.5 V corresponding to a maximum error of ± 0.05 V per cell. The minimization function is then kept running until all individual errors are under fixed threshold and the voltage profile is correctly followed by the model.

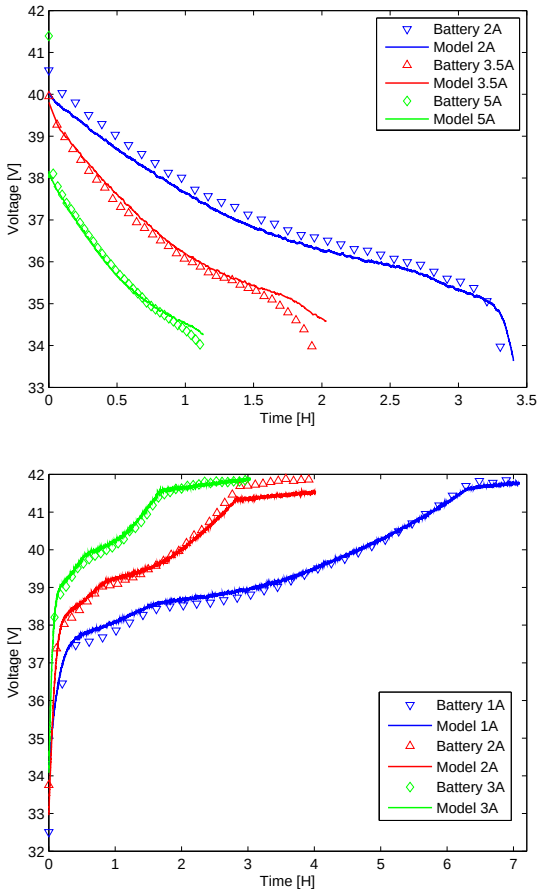

Fig. 4. Battery measurement versus battery model during identification test experiment. Upper plot shows discharge experiments, while bottom plot shows charge experiments.

V. Simulation Results

After the identification procedure the reduced order model exhibits a good voltage prediction, with a mean error about of 0.2 V and a maximum error under the chosen threshold. The resulting parameters values are listed in Table III. Figure 4 shows the obtained voltage prediction under charge and discharge at different rates, during the model identification process. The solid lines represent the model output, while the

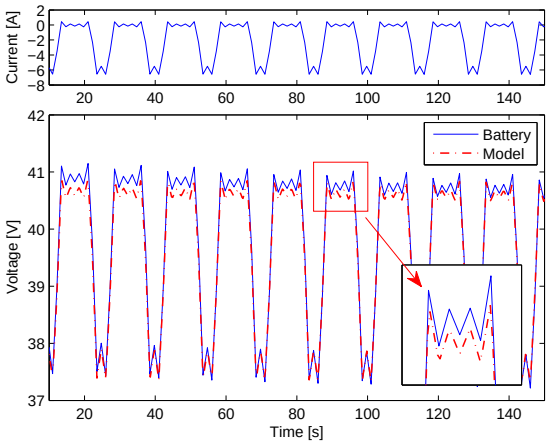

Fig. 5. Battery measurement versus battery model during identification test experiment, under pulse current discharge.

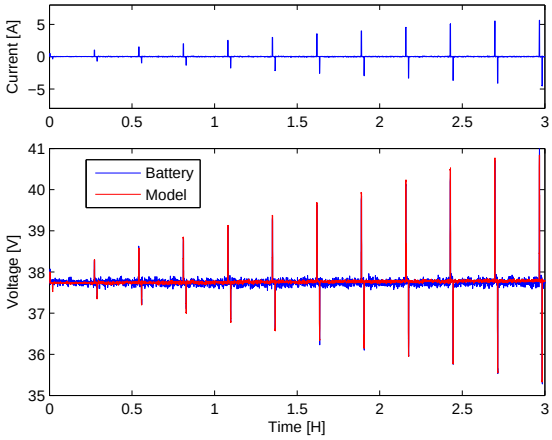

Fig. 6. Battery measurement versus battery model during validation test experiment, under repeated HPPC current demand profile.

marks represent experimental data. The simulations show a good agreement under all conditions and particularly god results away from the initiation and the termination of the experiments. During the initiation and the termination phase of its experiments, the internal battery protection circuitry is activated, hence it cause nonlinear phenomena which are not modeled.

Figure 5 shows the identification procedure results on a pulse operation discharge. For visualization reason, only the first 150 s of the simulation are shown, but results are representative of the entire test. The fast transients are followed without errors, showing good dynamic performances.

Finally the model has been validated on a different data set, not utilized for identification purpose. The current demand profile used for validation purpose is a series of ten Hybrid Pulse Power Characterization profiles (HPPC), as indicated in the FreedomCar manual [6]. Each HPPC profile lasts 60 s with reference current demand increases of 0.5 A (starting from 0.5 A up to 5.5 A), and is followed by 15min relaxation period. Figure 6 shows the complete simulation, while Figure 7 zoom only in a selection of the signal, in order to best illustrate the result. The battery measurement has been under sampled in order to improve readability of the figure.

Finally, in order to provide a SOC computation method, let us define the state of charge of the battery, with a good approximation, as linearly varying with θ between the two reference values at 0% and 100%

$$SOC(t) = \frac{\theta_x - \theta_x^{0\%}}{\theta_x^{100\%} - \theta_x^{0\%}}. \tag{18}$$

with $x = p, n$ for the positive and negative electrode. The SOC is then calculated using positive stoichiometry, because the model is more sensitive to positive solid concentration in respect to negative. Reference values for $\theta_p^{100\%}$ and $\theta_p^{0\%}$ have been taken from literature, and then refined to fit experimental data.

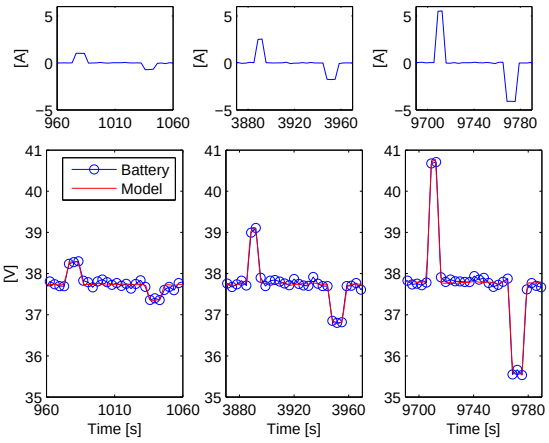

Fig. 7. Detail on selections of validation test experiment.

Figure 8 shows the estimated SOC for the validation experiment during one of the HPPC transient, in comparison with the SOC obtained from classic integrator definition. It is possible to notice how the proposed SOC estimation is able to take into account the concentration dynamics during fast transient, while the classic definition, based only on coulomb counting does not take into account the battery concentration dynamics.

VI. Conclusion

Identification of a battery model for SOC prediction has been performed. The results are illustrated and discussed, comparing the model outputs with the battery measurements. The battery model has been then validated using several set of data and a good performance of the identified model in predicting the experiment results is reached. Finally, a SOC estimation method has been presented and illustrated and its results confronted with classic integrator SOC computation.

Parameter	Negative electrode	Separator	Positive electrode
Thickness (cm)	$\delta_n = 50 \times 10^{-4}$ (b)	$\delta_{sep} = 20 \times 10^{-4}$ (a)	$\delta_p = 36.4 \times 10^{-4}$ (b)
Particle radius R_s (cm)	1×10^{-4} (a)	-	1×10^{-4} (a)
Active material volume fraction ε_s	0.580 (a)	-	0.500 (a)
Electrolyte phase volume fraction (porosity) ε_e	0.332 (b)	0.5 (b)	0.330 (b)
Charge transfers coefficients α_a, α_c	0.5,0.5 (b)	-	0.5, 0.5 (b)
Initial stoichiometry x_0,y_0	0.7 (b)	-	0.32 (b)

TABLE II

BATTERY PARAMETERS. (a) from battery datasheet, (b) from literature

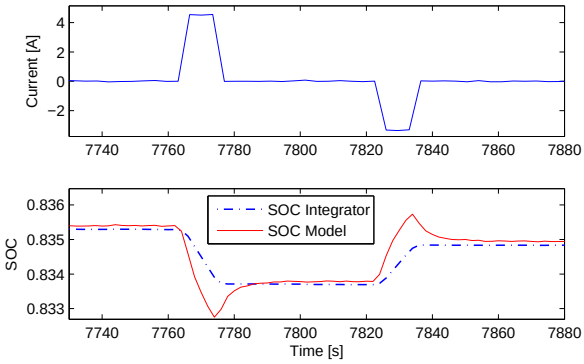

Fig. 8. Battery estimated SOC during an HPPC profile transient.

Name	Symbol and Value
Max negative solid concentration *(mol cm^{-3})*	$c_{s,max,n} = 3.175 \times 10^{-2}$
Max positive solid concentration *(mol cm^{-3})*	$c_{s,max,p} = 2.59 \times 10^{-2}$
Solid phase neg. diffusion coefficient *($cm^2\ s^{-1}$)*	$D_{s,n} = 1.27 \times 10^{-12}$
Solid phase pos. diffusion coefficient *($cm^2\ s^{-1}$)*	$D_{s,p} = 8.09 \times 10^{-12}$
Negative active surface area per electrode ($cm^2 cm^{-3}$)	$a_{s,n} = 9.655 \times 10^4$
Positive active surface area per electrode ($cm^2 cm^{-3}$)	$a_{s,p} = 2.425 \times 10^4$
Electrode plate Area cm^2	$A = 8000$
Total resistance (internal and external) Ωcm^2	$K_r = 128$
Current density coefficient	$k_0 = 1.918 \times 10^3$

TABLE III

PARAMETERS IDENTIFIED.

REFERENCES

[1] D. Di Domenico, G. Fiengo, and A. Stefanopoulou. Lithium-ion battery state of charge estimation with a kalman filter based on a electrochemical model. *Proceedings of 2008 IEEE Conference on Control Applications*, 1:702 – 707, 2008.

[2] D. Di Domenico, A. Stefanopoulou, and G. Fiengo. Reduced order lithium-ion battery electrochemical model and extended kalman filter state of charge estimation. *ASME Journal of Dynamic Systems, Measurement and Control - Special Issue on Physical System Modeling*, 2008.

[3] M. Doyle and Y. Fuentes. Computer simulations of a lithium-ion polymer battery and implications for higher capacity next-generation battery designs. *J. Electrochem. Soc.*, 150:A706–A713, 2003.

[4] M. Doyle, T.F. Fuller, and J. Newman. Modeling of galvanostatic charge and discharge of the lithium/polymer/insertion cell. *J. Electrochem. Soc.*, 140:1526–1533, 1993.

[5] W.B. Gu and C.Y. Wang. Thermal and electrochemical coupled modeling of a lithium-ion cell. *Proceedings of the ECS*, 99:748–762, 2000.

[6] U.S. Department of Energy. Freedomcar battery test manual for power-assist hybrid elecric veicles. *DOE/ID-11069*, 2003.

[7] V. Pop, H. J. Bergveld, J. Veld, P. Regtien, D. Danilov, and P. Notten. Modeling battery behavior for accurate state-of-charge indication. *J. Electrochem. Soc.*, 153:A2013–A2022, 2006.

[8] A.J. Salkind, C. Fennie, P. Singh, T. Atwater, and D.E. Reisner. Determination of state-of-charge and state-of-health of batts. by fuzzy logic methodology. *J. Power Sources*, 80:293–300, 1999.

[9] W.E. Schiesser. *The Numerical Method of Lines: Integration of Partial Differential Equations*. Elsevier Science & Technology, 1991.

[10] K. Smith and C.Y. Wang. Solid-state diffusion limitations on pulse operation of a lithium-ion cell for hybrid electric vehicles. *Journal of Power Sources*, 161:628–639, 2006.

[11] P. De Vidts, J. Delgado, and R.E. White. Mathematical modeling for the discharge of a metal hydride electrode. *J. Electrochem. Soc.*, 142:4006–4013, 1995.

[12] C.Y. Wang, W.B. Gu, and B.Y. Liaw. Micro-macroscopic coupled modeling of batteries and fuel cells. part i: Model development. *J. Electrochem. Soc.*, 145:3407–3417, 1998.

[13] C.Y. Wang, W.B. Gu, and B.Y. Liaw. Micro-macroscopic coupled modeling of batteries and fuel cells. part ii: Application to ni-cd and ni-mh cells. *J. Electrochem. Soc.*, 145:3418–3427, 1998.